Spin- and charge-density waves around Ru impurities in α-Fe alloys studied by ^{57}Fe Mössbauer spectroscopy

A. Błachowski,[1] K. Ruebenbauer,[1,*] and J. Żukrowski[2]

[1]*Mössbauer Spectroscopy Division, Institute of Physics, Pedagogical University, PL-30-084 Cracow, ulica Podchorążych 2, Poland*

[2]*Solid State Physics Department, Faculty of Physics and Applied Computer Science, AGH University of Science and Technology, PL-30-059 Cracow, Aleja Mickiewicza 30, Poland*

A random solid solution of ruthenium in the α-iron has been investigated by means of the Mössbauer spectroscopy using 14.4 keV transition in ^{57}Fe. Measurements were performed at room temperature versus ruthenium concentration varying up to about 12 at. %. Contributions to the iron hyperfine magnetic field and isomer shift due to the ruthenium impurity located at various distances from the resonant iron atom were determined. It was found that these contributions vary in sign depending upon the actual distance from the iron atom. The nearest neighbor ruthenium atom contributes −1.99 T. On the other hand, the second neighbor contributes −0.09 T, while the third neighbor contributes +0.52 T. Corresponding contributions to the isomer shift are as follows: −0.019, +0.072, and +0.005 mm/s. The above behavior is a strong indication for the presence of the spin and charge density waves in the vicinity of the ruthenium impurity in the α-iron.

PACS number(s): 75.50.Bb, 75.30.Fv, 71.45.Lr, 76.80.+y

I. INTRODUCTION

Mössbauer spectroscopy is sensitive to the local environment of the resonant atom. In particular one can study electron charge and spin density on the resonant nucleus, and perturbations of the above densities due to some impurity located close to the resonant atom.[1,2] Impurities randomly dissolved on the regular sites of the bcc ferromagnetic α-iron have an effect on the density of the s-like electrons in their vicinity, and hence they perturb the observed isomer shift. A corresponding perturbation of the spin density of the s-like electrons has influence on the hyperfine field via modification of the transferred field. In the majority of cases the above perturbations are seen up to the third nearest neighbor shell at most.[3,4]

II. EXPERIMENTAL

Samples were prepared by arc melting of the appropriate amounts of the natural iron of the 99.97+ at. % purity and natural ruthenium of the 99.9 at. % purity. Approximately 1.5 g samples were prepared. The samples were melted three times under high purity argon in order to achieve high homogeneity. The concentration of ruthenium was determined by means of the electron microprobe for each sample. Resulting ingots were used to produce powder by using a diamond file. Approximately 150 mg of powder was made from each ingot.[5] The lattice constant was determined at room temperature by means of the x-ray powder diffraction for the pure iron used to prepare samples and for the sample having 8.50 at. % of ruthenium; i.e., for the last sample being well within the single phase range.[6] The Cu $K\alpha_{1,2}$ radiation monochromatized by means of the pyrolytic graphite monochromator was used. The sample was mixed with the high purity tungsten powder the latter used to calibrate precisely the scattering angle scale. Mössbauer spectra were obtained at room temperature in a standard transmission mode using commercial ^{57}Co(Rh) source kept at room temperature as

well. The MsAa-3 spectrometer was used[7] with 4096 channels per raw unfolded spectrum obtained in the linear round-corner mirror mode. Approximately 30 mg/cm^2 of the investigated alloy was used while preparing absorbers. All spectral
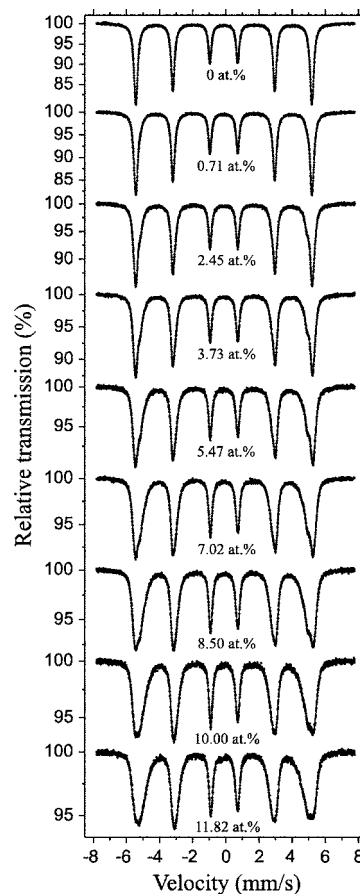
FIG. 1. Mössbauer spectra for various ruthenium concentrations plotted versus absolute velocity. The solid line represents fit to the $\sigma=3$ model.

TABLE I. Essential parameters obtained for the model with $\sigma=2$. The last row shows respective averages, where applicable.

c (at. %)	$\langle B \rangle_2$ (T) ±0.02	$B_0^{(2)}$ (T) ±0.02	ΔB_1 (T) ±0.02	ΔB_2 (T) ±0.02	$\langle S \rangle_2$ (mm/s) ±0.002	$S_0^{(2)}$ (mm/s) ±0.002	ΔS_1 (mm/s) ±0.002	$\langle \Delta S \rangle_2$ (mm/s) ±0.002
0	32.97				0			
0.71 (1)	32.88	32.96	−1.93	0.72	0.002	0.003	−0.019	0.007
2.45 (2)	32.74	33.01	−1.87	0.76	0.004	0.007	−0.018	0.005
3.73 (2)	32.64	33.06	−1.89	0.78	0.008	0.013	−0.017	0.003
5.47 (3)	32.49	33.11	−1.92	0.79	0.011	0.018	−0.018	0.005
7.02 (3)	32.30	33.11	−1.95	0.81	0.015	0.024	−0.017	0.003
8.50 (4)	32.16	33.13	−1.98	0.81	0.018	0.028	−0.016	0.003
10.00 (6)	31.92	33.09	−2.02	0.82	0.021	0.032	−0.016	0.003
11.82 (8)	31.67	33.06	−2.04	0.83	0.024	0.042	−0.017	-0.002
		33.07	**−1.95**	**0.79**		**0.021**	**−0.017**	**0.003**

shifts are reported here versus shift of the α-iron kept at room temperature. A velocity scale of the spectrometer was calibrated using high purity α-iron kept at room temperature.

III. DATA EVALUATION

Folded Mössbauer spectra were evaluated within the transmission integral approximation[8] using previously developed model.[4,5] Results are shown in Fig. 1. The basic assumptions of the above model are as follows. It is assumed that impurities are located randomly on the regular lattice sites of the α-iron, and that perturbations caused by various impurities are additive in the algebraic sense. On the other hand, particular perturbations depend solely on the distance from the observation point; i.e., from the resonant nucleus. Therefore, one can define a contribution to the hyperfine field ΔB_s due to the impurity located in the sth coordination shell of the resonant atom, and a corresponding contribution ΔS_s to the isomer shift; i.e., to the spin and charge density perturbation, respectively. One has to take into account all shells around the resonant atom until the most distant shell having measurable effect. Usually it is either the second or

the third coordination shell labeled by the index σ. More distant shells contribute to the remainder of the hyperfine field $B_0^{(\sigma)}$ and spectral shift $S_0^{(\sigma)}$. The average field $\langle B \rangle_\sigma$ and the average shift $\langle S \rangle_\sigma$ could be obtained in a straightforward manner under the above assumptions.[5] Results are shown versus ruthenium concentration c in Table I for $\sigma=2$ model and in Table II for $\sigma=3$ model. The sample with the highest concentration of ruthenium (11.82 at. %) exhibits about 1.6% contribution to the absorption cross section due to the paramagnetic fcc γ-FeRu phase.[6,9] This contribution is well described by the broad singlet having −0.2 mm/s spectral shift.[9]

Mössbauer data were independently processed by the Hesse-Rübartsch method[10,11] in the thin absorber approximation applied to the hyperfine magnetic fields, i.e., a distribution of the hyperfine magnetic fields was fitted to the data, while the spectral shift was kept common for all subspectra. The average fields $\langle B \rangle$ and the shifts $\langle S \rangle$ obtained by this method are shown versus ruthenium concentration in Table III.

Lattice constants were determined by the Rietveld fit to the respective x-ray diffraction patterns. The following re-

TABLE II. Essential parameters obtained for the model with $\sigma=3$. The last row shows respective averages, where applicable.

c (at. %)	$\langle B \rangle_3$ (T) ±0.02	$B_0^{(3)}$ (T) ±0.02	ΔB_1 (T) ±0.02	ΔB_2 (T) ±0.02	ΔB_3 (T) ±0.02	$\langle S \rangle_3$ (mm/s) ±0.002	$S_0^{(3)}$ (mm/s) ±0.002	$\langle \Delta S \rangle_1$ (mm/s) ±0.002	$\langle \Delta S \rangle_2$ (mm/s) ±0.002	$\langle \Delta S \rangle_3$ (mm/s) ±0.002
0	32.97					0				
0.71 (1)	32.88	32.95	−1.95	0.02	0.42	0.003	0.000	−0.020	0.096	0.000
2.45 (2)	32.74	32.97	−1.92	−0.03	0.50	0.006	−0.002	−0.019	0.078	0.002
3.73 (2)	32.63	32.98	−1.95	−0.03	0.53	0.010	−0.002	−0.019	0.075	0.001
5.47 (3)	32.47	33.01	−1.97	−0.08	0.53	0.013	−0.005	−0.020	0.072	0.005
7.02 (3)	32.29	32.98	−2.00	−0.08	0.55	0.017	−0.005	−0.019	0.070	0.004
8.50 (4)	32.14	33.02	−2.02	−0.14	0.55	0.020	−0.009	−0.018	0.065	0.008
10.00 (6)	31.90	33.00	−2.04	−0.22	0.55	0.021	−0.013	−0.019	0.060	0.011
11.82 (8)	31.65	32.93	−2.06	−0.18	0.56	0.025	−0.011	−0.019	0.062	0.007
		32.98	**−1.99**	**−0.09**	**0.52**		**−0.006**	**−0.019**	**0.072**	**0.005**

TABLE III. Average hyperfine field and spectral shift obtained versus ruthenium concentration by means of the Hesse-Rübartsch method.

c (at. %)	0	0.71 (1)	2.45 (2)	3.73 (2)	5.47 (3)	7.02 (3)	8.50 (4)	10.00 (6)	11.82 (8)
$\langle B \rangle$ (T) ± 0.02	33.02	32.91	32.75	32.64	32.48	32.30	32.15	31.92	31.67
$\langle S \rangle$ (mm/s) ± 0.002	0	0.002	0.006	0.008	0.011	0.016	0.019	0.020	0.024

sults were obtained: $a=2.8673(2)$ Å for pure iron and $a=2.8895(2)$ Å for the sample having 8.50 at. % ruthenium.

IV. DISCUSSION OF RESULTS

Figure 2 shows essential parameters of the data evaluation model described above[4,5] plotted versus ruthenium concentration. The average fields and shifts are quite similar for models with $\sigma=2$ and $\sigma=3$. On the other hand, the parameters $B_0^{(\sigma)}$ and $S_0^{(\sigma)}$ indicate that the model with $\sigma=3$ has sufficient number of the individual coordination shells taken into account, while the model with $\sigma=2$ is insufficient to describe properly perturbations caused by impurities at various distances. Corresponding distributions of the hyperfine magnetic field B are plotted in Fig. 3 and compared with distributions following Hesse-Rübartsch data treatment

results.[10,11] Distributions of the $\sigma=3$ model are quite similar to the distributions obtained by the Hesse-Rübartsch method for higher ruthenium concentrations. The same statement applies to the average fields and shifts. A discrepancy at low ruthenium concentrations is due to the lack of the physical background in the Hesse-Rübartsch approach. Hence, one cannot detect oscillatory character of the perturbations basing on the Hesse-Rübartsch data evaluation.

FIG. 2. The most relevant model parameters plotted versus ruthenium concentration.
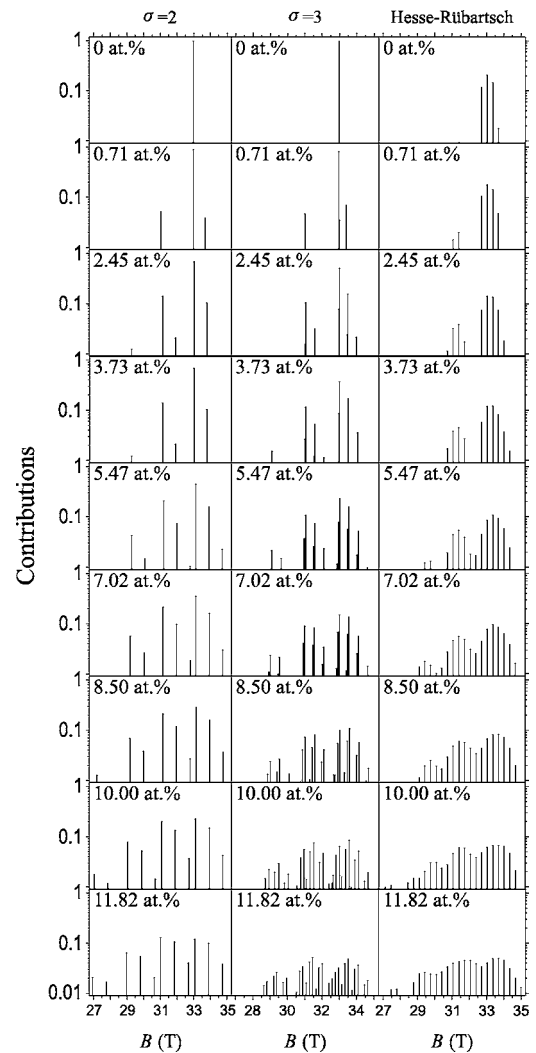
FIG. 3. Hyperfine field distributions are plotted for various ruthenium concentrations and compared with the distributions obtained by the Hesse-Rübartsch method.
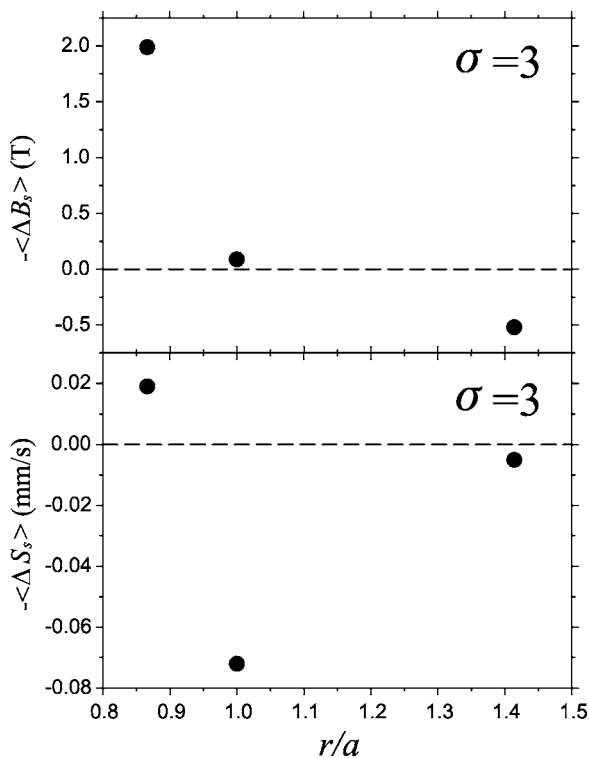
FIG. 4. Electron spin density perturbation due to the ruthenium impurity and corresponding electron density perturbation plotted versus relative distance from the mean position of the impurity. Data were averaged over all nonzero ruthenium concentrations investigated.

Figure 4 shows the parameters $-\langle \Delta B_s \rangle$ and $-\langle \Delta S_s \rangle$ plotted versus relative distance r/a from the mean position of the ruthenium impurity. Here the symbol r stands for the distance from the mean position of the ruthenium impurity. The above parameters were obtained within the $\sigma = 3$ model. The first parameter is directly proportional to the perturbation of the transferred electron spin density, while the second one is proportional to the perturbation of the transferred electron density provided the second order Doppler shift remains unaffected by addition of the impurities. The sign of the perturbation in the transferred electron spin density is defined against the sign of the spin density of the electrons constituting the core of the iron ion. The absolute distance scale could be easily calculated using the above quoted lattice constants as the Vegard law is well satisfied for the ruthenium concentration range involved.[12,13] The averaging was performed over all nonzero concentrations of ruthenium as shown in Table II. It is obvious that the perturbations of the electron spin density and electron (negative electric charge) density around the ruthenium atom in the α-iron have character of the damped oscillations, i.e., such impurity generates some spin and charge density waves in its vicinity, while embedded in the α-iron. It seems that *quasi*periods of these two types of waves are rather dissimilar. No electric quadrupole interaction due to the presence of the ruthenium impurities in the α-iron was detected on the iron nuclei for the ruthenium concentration range investigated.

Similar investigations have been previously performed for the following impurities in the α-iron: Pd,[4] Os,[14] and Nb.[5]

Neither perturbations of the charge nor the perturbations of the spin densities were found to exhibit oscillations.

No electric quadrupole interaction in the excited state of the iron resonant nucleus was detected for any of the subspectra giving measurable contributions to the total spectrum. The same statement actually applies to the systems investigated previously; i.e., to the α-iron doped with Pd,[4] Os,[14] and Nb.[5] The accuracy of the data warrants detection of the particular line shift caused by the electric quadrupole interaction provided the latter shift is of the order of 0.1 mm/s or larger and the line has sufficient intensity to be observable. The reasons for such behavior are as follows, in our opinion. First of all there is no electric quadrupole interaction in the pure α-iron due to the symmetry. Impurities located at larger distances than the first coordination shell make a negligible contribution owing to the very strong screening by the conduction electrons. The strongest interactions are expected for a single defect in the first coordination shell and linear defects of the Ru-Fe-Ru and Fe-Fe-Fe types, as other defect configurations are screened by the conduction electrons to a large extent.[15] There are two such single-defect configurations; i.e., the ruthenium atom and seven iron atoms, or seven ruthenium atoms and a single iron atom. The latter configuration makes a negligible contribution to the spectrum at the ruthenium concentrations investigated here. On the other hand, these single-defect configurations generate an axially symmetric electric field gradient with the principal axis pointing in one of the equivalent $\langle 111 \rangle$ directions within the unit cell. Linear defects of the Fe-Fe-Fe type are very rare at the ruthenium concentrations involved, as they require remaining six vortices of the nearest neighbor shell to be filled by ruthenium atoms. Linear defects produce an axially symmetric electric field gradient with the principal axis pointing in one of the equivalent $\langle 111 \rangle$ directions. It has to be noted that the electric quadrupole interaction is invariant upon the spatial inversion. The easy axis of magnetization points along one of the main directions of the unit cell in the α-iron. The hyperfine field on the iron nucleus is oriented opposite to the abovementioned direction, as the total Fermi contact term is fairly isotropic. The electric quadrupole interaction is small compared to the corresponding magnetic dipole interaction for all relevant defect configurations, and therefore it is described by the first order perturbation term. The latter term is proportional to $3\cos^2 \vartheta - 1$ (see Ref. 16) with the symbol ϑ denoting the angle between the hyperfine field direction and the direction of the electric field gradient principal axis. This term vanishes for the unperturbed lattice and it is expected to be very small for the relaxed chemical and magnetic lattices due to the presence of the impurity or the linear defect of the Ru-Fe-Ru type. In principle one can look for some electric quadrupole interactions above the Curie point, but the Curie temperature for the iron-ruthenium system investigated here is high enough to cause some decomposition of the alloy during the spectrum accumulation.[6]

The oscillatory behavior detected in the iron-ruthenium system is probably similar to the behavior in the metallic chromium.[17] The latter system is characterized by the significant contribution to the spin and charge density due to the itinerant electrons. These electrons exhibit incommensurate oscillations of the charge and spin densities in comparison

with the lattice period. Probably the iron-ruthenium system behaves similarly. Recent *ab initio* calculations performed by Spišák *et al.*[18] have shown that the ruthenium magnetic moment depends strongly upon the lattice constant indicating some tendency to form itinerant spin polarization. These calculations were performed for hexagonal iron-ruthenium multilayers. Hence, there is a need to perform similar calculations for the ruthenium impurity embedded in the α-iron. Impurities investigated by us previously (Pd, Os, and Nb) do not exhibit such itinerant behavior to our best knowledge. Actually, many old models of the magnetic interactions between atomic spins predicted oscillatory behavior of the spin density.[19] However, these models were unsatisfactory as they relied upon almost free electron Fermi gas with perturbations introduced locally in a very approximate way.

*Corresponding author: sfrueben@cyf-kr.edu.pl

[1] J. Cieślak and S. M. Dubiel, J. Alloys Compd. **350**, 17 (2003).

[2] I. Vincze and I. A. Campbell, J. Phys. F: Met. Phys. **3**, 647 (1973).

[3] J. Korecki and U. Gradmann, Phys. Rev. Lett. **55**, 2491 (1985).

[4] A. Błachowski, K. Ruebenbauer, and J. Żukrowski, Phys. Scr. **70**, 368 (2004).

[5] A. Błachowski, K. Ruebenbauer, and J. Żukrowski, Phys. Status Solidi B **242**, 3201 (2005).

[6] T. B. Massalski, *Binary Alloy Phase Diagrams*, 2nd ed. (ASM International, Materials Park, Ohio, 1990), Vol. 1, p. 1764.

[7] R. Górnicki, RENON, http://www.renon.strefa.pl

[8] S. Margulies, P. D. Debrunner, and H. Frauenfelder, Nucl. Instrum. Methods **21**, 217 (1963).

[9] S. Gupta, K. B. Lal, T. M. Srinivasan, and G. N. Rao, Phys. Status Solidi A **22**, 707 (1974).

[10] J. Hesse and A. Rübartsch, J. Phys. E **7**, 526 (1974).

[11] G. Le Caër and J. M. Dubois, J. Phys. E **12**, 1083 (1979).

[12] M. Hada, K. Sumiyama, and Y. Nakamura, Phys. Status Solidi A **108**, 295 (1988).

[13] W. B. Pearson, *A Handbook of Lattice Spacings and Structures of Metals and Alloys* (Pergamon, Oxford, 1967), Vol. 2, p. 928.

[14] A. Błachowski, K. Ruebenbauer, and J. Żukrowski, Nukleonika **49**, S67 (2004).

[15] Y. Yoshida, F. Langmayr, P. Fratzl, and G. Vogl, Phys. Rev. B **39**, 6395 (1989).

[16] N. N. Greenwood and T. C. Gibb, *Mössbauer Spectroscopy* (Chapman and Hall Ltd., London, 1971), p. 63.

[17] S. M. Dubiel, J. Cieślak, and F. E. Wagner, Phys. Rev. B **53**, 268 (1996).

[18] D. Spišák, R. Lorenz, and J. Hafner, Phys. Rev. B **63**, 094424 (2001).

[19] J. Sakurai, Y. Kubo, T. Kondo, J. Pierre, and J. Bertaud, J. Phys. Chem. Solids **34**, 1305 (1973).